

Theoretical investigation of resonant multiple Auger decay of the core-excited $2p_{3/2}^{-1}4s$ state in argon

Yulong Ma,¹ Zhenqi Liu,¹ Fuyang Zhou,² and Yizhi Qu^{1,*}

¹*School of Optoelectronics, University of Chinese Academy of Sciences, Beijing 100049, China*

²*Data Center for High Energy Density Physics, Institute of Applied Physics and Computational Mathematics, Beijing 100088, China*



(Received 3 August 2018; published 10 October 2018)

The resonant single, double, triple, and quadruple Auger decays of the core-excited Ar $2p_{3/2}^{-1}4s$ are investigated by using the multistep approaches, i.e., the cascade, knock-out, and shake-off mechanisms within the framework of many-body perturbation theory. The Auger rates, the branching ratios for the different configurations in the final ions and the probabilities of the spectator, participator, and shake processes, as well as the ion yields are obtained. The cascade processes are dominant in the resonant double Auger decay since the initial Rydberg electron $4s$ preferentially remains in its orbital as a spectator in the primary resonant single Auger decay. In the direct processes, the spectator processes are essential for the populations of final states, while the participator processes become dominant as the number of emitted Auger electrons increases, especially for the resonant quadruple Auger decay. Furthermore, the shake processes also affect significantly the final states for the direct processes. The calculated ion yields (in percentages) of Ar⁺, Ar²⁺, Ar³⁺, and Ar⁴⁺ of 65.3, 31.0, 3.6, and 0.09, respectively, are in agreement with the recent experimental values of 69, 28, 3, and 0.03 [Hikosaka *et al.*, *Phys. Rev. A* **89**, 023410 (2014)] and 66, 30, 4, and 0.2 [Samson *et al.*, *Phys. Rev. A* **54**, 2099 (1996)].

DOI: [10.1103/PhysRevA.98.043417](https://doi.org/10.1103/PhysRevA.98.043417)

I. INTRODUCTION

Resonant Auger decays of a core-excited state produced by exciting an inner-shell electron to a Rydberg orbital may emit one, two, and even more Auger electrons. The resonant multiple Auger (RMA) decay is one of the important relaxation processes for the inner-shell excited atom upon radiationless decays, which results from the many-electron Coulomb interaction. Therefore, investigations of such processes could give important information on electron correlation effects and many-body problems in atomic processes [1,2]. As a high-order process, RMA decay is forbidden within the independent particle model (frozen atomic structure approximation) and, hence, it is a good candidate for testing the theoretical models that incorporate electron correlations in such process. Furthermore, studying the interplay of Auger processes offers valuable information on the electronic structure of atoms and molecules as well as the electron dynamics underlying high-charge-state formation [3,4] and hollow atoms [5–7].

Many experimental and theoretical efforts have been made involving the RMA decays [8–11]. Specifically, if an electron in the relativistic $2p_{3/2}$ shell of a neutral Ar atom is excited to an empty shell such as $4s$, the RMA decays are energetically allowed with the emission of at least two Auger electrons [9–11]. Samson *et al.* [9] have measured partial cross sections for Ar⁺ through Ar⁴⁺ with the photon energy range from 242 to 253 eV, and the ion yields are deduced for Ar⁺, Ar²⁺, Ar³⁺, and Ar⁴⁺ to be 66, 30, 4, and 0.2, respectively. Hikosaka *et al.* [10] measured spectra displaying the Ar²⁺ states populated

by the direct resonant double Auger (RDA) decay following $2p$ core-electron excitation. They demonstrated that the shake-off (SO) mechanism is not sufficient, and the knock-out (KO) mechanism should also be included for theoretically describing the direct RDA decay. Recently, Hikosaka *et al.* [11] investigated more comprehensively the RMA decays for the Ar $2p_{3/2}^{-1}4s$ with the multielectron coincidence method, and illustrated the contributions of the cascade and direct processes as well as the spectator and participator behavior of the initial Rydberg electron.

In the resonant Auger decay, the Rydberg electron can (i) remain in its orbital as a spectator, (ii) take part in the Auger process, or (iii) be shaken up to a higher or shaken down to a lower orbital, which refer to spectator, participator, and shake processes, respectively. These processes from Ar $2p_{3/2}^{-1}4s$ can be represented as follows:

$$2p_{3/2}^{-1}3s^23p^64s \rightarrow 2p^6(3s3p)^{7-q}4s + qe^-$$

(spectator process), (1)

$$2p_{3/2}^{-1}3s^23p^64s \rightarrow 2p^6(3s3p)^{8-q} + qe^-$$

(participator process), (2)

$$2p_{3/2}^{-1}3s^23p^64s \rightarrow 2p^6(3s3p)^{7-q}nl + qe^-(nl \neq 4s)$$

(shake process), (3)

where $q = 1, 2, 3$, and 4 correspond to the resonant single Auger (RSA), RDA, resonant triple Auger (RTA), and resonant quadruple Auger (RQA) decays, respectively. For the RSA decay, these processes play a crucial role in determining

*yzqu@ucas.ac.cn

the populations of final states and have been studied extensively [12–16], in which the spectator process usually is most favored. However, detailed theoretical studies on the behavior of the initial Rydberg electron are still needed for the RMA decay of the Ar $2p_{3/2}^{-1}4s$.

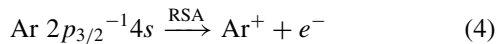
In this paper, we present a theoretical study on the RMA decays including the cascade and direct processes for the Ar atom with a $2p_{3/2}$ hole following the resonant $2p_{3/2} \rightarrow 4s$ photoexcitation. In particular, the spectator, participator, and shake processes, related to the behavior of the initial Rydberg electron $4s$ in the RMA decay, are explored for the populations of the final states. In order to obtain the RMA rates, the multistep approaches derived from many-body perturbation theory (MBPT), namely, cascade, KO, and SO mechanisms, are employed. According to the Auger rates, we are able to present the Auger spectra; probabilities of the spectator, participator, and shake processes; as well as ion yields, which are consistent with the experimental data [9,11].

II. THEORY

The initial state Ar $2p_{3/2}^{-1}4s$ that lies above the Ar⁺, Ar²⁺, Ar³⁺, and Ar⁴⁺ thresholds can decay via the RSA, RDA, RTA, and RQA decays. For the RMA decay, the emission of many electrons can be simultaneous, or it can proceed in a stepwise manner through the creation and decay of an intermediate autoionizing state, which are referred to as the direct and cascade processes, respectively.

A. Resonant single Auger decay

The rate of the RSA decay of the initial $2p_{3/2}^{-1}4s$ state resulting in the final Ar⁺ states with the emission of one Auger electron



can be expressed as [17,18]

$$A_{if}^{\text{SA}} = \left| \langle \psi_f^+, \kappa; J_T M_T | \sum_{p < q} \frac{1}{r_{pq}} | \psi_i \rangle \right|^2, \quad (5)$$

where $|\psi_i\rangle$ represents the initial autoionizing state and $|\psi_f^+, \kappa; J_T M_T\rangle$ is the final ionic state $|\psi_f^+\rangle$ plus a continuum Auger electron with the relativistic angular quantum number κ . J_T and M_T are the total angular momentum and magnetic quantum number of the final state, respectively.

B. Resonant double Auger decay

In the direct RDA decay, two Auger electrons are emitted simultaneously:



In our previous work [19,20], the KO and SO mechanisms derived from the MBPT [21] are employed to obtain the direct double Auger rates. Thus, the direct RDA rate can be obtained

by sum of the two mechanisms, which are expressed as

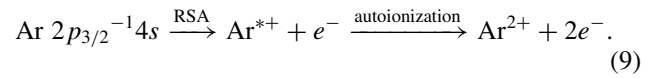
$$A_{if}^{\text{DDA(KO)}} = \sum_m A_{im}^{\text{SA}} \Omega_{mf}(\varepsilon_0), \quad (7)$$

$$A_{if}^{\text{DDA(SO)}} = \sum_m A_{im}^{\text{SA}} |\langle \psi_f^{2+}, \kappa; J_T M_T | \psi_m^+ \rangle|^2, \quad (8)$$

respectively. Here A_{im}^{SA} is the RSA rate for the initial state Ar $2p_{3/2}^{-1}4s$ to the intermediate Ar⁺ states. $\Omega_{mf}(\varepsilon_0)$ is the collision strength of the inelastic scattering by the “intermediate” Auger electron with energy ε_0 from the primary RSA process, and the matrix element $\langle \psi_f^{2+}, \kappa; J_T M_T | \psi_m^+ \rangle$ represents the overlap integral between the intermediate state Ar⁺ and final ionic state Ar²⁺ with the second Auger electron.

In the KO mechanism, the second Auger electron can be knocked out from the intermediate Ar⁺ ion through inelastic scattering by the first Auger electron with specific energy and angular momentum from the primary RSA decay. The SO mechanism emits the second Auger electron following a sudden change of the atomic potential caused by the rapid ejection of the primary RSA electron. Therefore, the KO and SO are referred to as the final-state correlation [22] due to the electron-electron interactions after the RSA decay.

In the cascade RDA decay, the initial state Ar $2p_{3/2}^{-1}4s$ can undergo a RSA decay to an intermediate autoionizing state Ar^{*+}, and then decay further to final Ar²⁺ states via the emission of another electron:



Then the cascade RDA rate can be obtained from

$$A_{if}^{\text{CDA}} = \sum_m A_{im}^{\text{SA}} A_{mf}^{\text{SA}} \Gamma_m^{-1}, \quad (10)$$

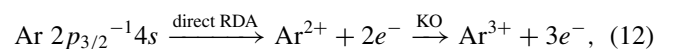
where A_{im}^{SA} and A_{mf}^{SA} are the single Auger rate for the first and second steps of the cascade RDA decay, respectively. Γ_m is the total width of the intermediate state Ar^{*+}.

C. Resonant triple Auger decay

For the RTA decay, the direct and cascade processes are also possible. The direct RTA decay results in the final Ar³⁺ states emitting three Auger electrons simultaneously:



We propose a multistep approach to deal with the direct RTA decay by including the final-state correlation with the KO mechanism after the direct RDA decay. Since the SO mechanism is weak for low energy [23], the additional final-state correlation from the SO mechanism is neglected after the direct RDA decay for the Auger electron energies below 200 eV. This is also true for the case of C $1s^{-1}$ [19] and Ne $1s^{-1}$ [20]. Then the direct RTA decay [Eq. (11)] can be decomposed into a sequence of the direct RDA process and the inelastic scattering process within the KO mechanism:



and, hence, the corresponding direct RTA rate can be obtained from the expression

$$A_{if}^{\text{DTA}} = \sum_m A_{im}^{\text{DDA}} \int_0^{E_{im}} \rho_{im}(\varepsilon) \Omega_{mf}(\varepsilon) d\varepsilon. \quad (13)$$

A_{im}^{DDA} is the rate of the primary direct RDA decay from the initial state $\text{Ar } 2p_{3/2}^{-1} 4s$ (with energy E_i) to the intermediate state of the Ar^{2+} ion (with energy E_m), which emits simultaneously two “intermediate” Auger electrons sharing the continuously distributed energy $E_{im} = E_i - E_m$. $\Omega_{mf}(\varepsilon)$ is the collision strength of inelastic scattering off a bound electron in the intermediate Ar^{2+} ion by one of the two “intermediate” Auger electrons, which has kinetic energy range from zero to E_{im} with symmetrical U-shape distribution [24,25]. This normalized distribution $\rho_{im}(\varepsilon)$ was approximately obtained by the binary-encounter (BE) model [26], the validity of which has been illustrated for the direct double Auger transition $\text{Ne } 1s^{-1} \rightarrow 2s^{-2} 2p^{-1} 2p$ [20].

In the cascade RTA decay, three Auger electrons are emitted in a stepwise manner through the creation and decay of intermediate autoionizing states such as Ar^{*+} and Ar^{*2+} , which can be considered in the following two categories:

$$\text{Ar } 2p_{3/2}^{-1} 4s \xrightarrow{\text{RSA}} \text{Ar}^{*+} + e^- \xrightarrow{\text{double autoionization}} \text{Ar}^{3+} + 3e^-, \quad (14)$$

$$\begin{aligned} \text{Ar } 2p_{3/2}^{-1} 4s &\xrightarrow{\text{direct RDA}} \text{Ar}^{*2+} + 2e^- \\ &\xrightarrow{\text{autoionization}} \text{Ar}^{3+} + 3e^-. \end{aligned} \quad (15)$$

In Eq. (14), the initial state $\text{Ar } 2p_{3/2}^{-1} 4s$ decays to the intermediate autoionizing states Ar^{*+} that lie above the Ar^{3+} threshold, via a primary RSA decay. Then these intermediate states can decay further to the Ar^{3+} states via a double autoionization with emission of two electrons. However, the energies of such states Ar^{*+} are so high that their populations are very limited, and the contributions of the subsequent double autoionization leading to final Ar^{3+} states are even smaller. Therefore, the cascade RTA decay (14) is negligible, which also has been proved in our test calculations.

Now, we mainly focus on the case (15), in which the final states Ar^{3+} are attributed to a primary direct RDA decay to an intermediate autoionizing state Ar^{*2+} lying above the Ar^{3+} threshold with a subsequent autoionization. Then the cascade RTA rate can be obtained with

$$A_{if}^{\text{CTA}} = \sum_m A_{im}^{\text{DDA}} A_{mf}^{\text{SA}} \Gamma_m^{-1}, \quad (16)$$

where A_{im}^{DDA} is the direct RDA rate of the initial state $\text{Ar } 2p_{3/2}^{-1} 4s$ to the intermediate autoionizing state Ar^{*2+} , and A_{mf}^{SA} represents the rate of further autoionization from the Ar^{*2+} states to the final state Ar^{3+} . Γ_m is the total width of the intermediate state Ar^{*2+} .

D. Resonant quadruple Auger decay

Similarly, the direct and cascade processes are also considered for the RQA decay. The initial state $\text{Ar } 2p_{3/2}^{-1} 4s$ decays

to final Ar^{4+} states via the direct RQA decay:

$$\text{Ar } 2p_{3/2}^{-1} 4s \xrightarrow{\text{direct RQA}} \text{Ar}^{4+} + 4e^-. \quad (17)$$

To describe the direct RQA decay, multistep approaches are proposed by including the important final-state correlation using the KO mechanism, while the weak SO mechanism is neglected. In this approach, similarly to the direct RTA decay, the direct RQA decay is the combination of a primary direct RTA decay and a subsequent KO mechanism:

$$\text{Ar } 2p_{3/2}^{-1} 4s \xrightarrow{\text{direct RTA}} \text{Ar}^{3+} + 3e^- \xrightarrow{\text{KO}} \text{Ar}^{4+} + 4e^-. \quad (18)$$

Based on a recent experimental finding about the direct triple Auger of core-ionized $\text{Ar } 2p^{-1}$, the energy of one of the three outgoing Auger electrons can be continuously distributed [27]. Therefore, it is safely assumed that one of the emitted electrons from the direct RTA decay is treated as incident for the inelastic scattering in the subsequent KO mechanism. The corresponding direct RQA rate is then given by

$$A_{if}^{\text{DQA}} = \sum_m A_{im}^{\text{DTA}} \int_0^{E_{im}} \rho_{im}(\varepsilon) \Omega_{mf}(\varepsilon) d\varepsilon, \quad (19)$$

where A_{im}^{DTA} and E_{im} are the transition rate and energy for the direct RTA decay from initial state $\text{Ar } 2p_{3/2}^{-1} 4s$ to the Ar^{3+} states, respectively. $\Omega_{mf}(\varepsilon)$ is the collision strength of the inelastic scattering off a bound electron in the intermediate Ar^{3+} ion by one of the intermediate Auger electrons with the energy distribution $\rho_{im}(\varepsilon)$ from zero to E_{im} . In our simple approaches, since the emission of Auger electrons in the direct process results mainly from final-state correlations of the electron-electron scattering (KO), the energy distribution of one Auger electron can be obtained by the BE model [26]. According to our separate test calculations, BE can approximately describe energy distribution of one Auger electron for the direct triple Auger transition $\text{Ar } 2p^{-1} \rightarrow 3p^{-4}$ [27].

There are some possible cascade RQA processes from the $2p_{3/2}^{-1} 4s$ to Ar^{4+} states, for example, through the multiple autoionization of intermediate autoionizing states such as Ar^{*+} and Ar^{*2+} created by the primary RSA and RDA decays, respectively. However, these intermediate states lying above the Ar^{4+} threshold are populated negligibly. Therefore, we restrict ourselves to another cascade process of four-electron emission, which results from the fact that three primary electrons are emitted simultaneously in the primary direct RTA decay of the initial state $\text{Ar } 2p_{3/2}^{-1} 4s$ populating into intermediate autoionizing states Ar^{*3+} , and then another electron is emitted due to the further autoionization of states Ar^{*3+} lying above the Ar^{4+} threshold,

$$\begin{aligned} \text{Ar } 2p_{3/2}^{-1} 4s &\xrightarrow{\text{direct RTA}} \text{Ar}^{*3+} + 3e^- \\ &\xrightarrow{\text{autoionization}} \text{Ar}^{4+} + 4e^-, \end{aligned} \quad (20)$$

and then the rate of the cascade RQA decay is given by

$$A_{if}^{\text{CQA}} = \sum_m A_{im}^{\text{DTA}} A_{mf}^{\text{SA}} \Gamma_m^{-1}, \quad (21)$$

TABLE I. Rates (A^1) and branching ratios (BR¹) for main configurations in Ar⁺ ions, as well as probabilities (P^1) of the spectator, participator, and shake processes of the resonant single Auger decay. The numbers in brackets represent powers of 10.

Ar ⁺	A^1 (s ⁻¹)	BR ¹ (%)	Final orbital	Process	P^1 (%)		
					Ours	Calc. [32]	Expt.
$3s^23p^5$	7.7(11)	0.3	$3s/3p$	Participator	0.3		
$3s3p^6$	2.7(10)	~0					
$3s^23p^43d$	3.5(13)	15.2	$3d$	Shake-down	15.4		
$3s3p^53d$	4.3(11)	0.2					
$3s^23p^44s$	1.2(14)	52.2	$4s$	Spectator	71.7		
$3s3p^54s$	2.5(13)	10.9					
$3p^64s$	2.8(12)	1.2					
$(3s3p)^54snl$	1.7(13)	7.4					
$3s^23p^45s$	2.3(13)	10.0	$5s$	Shake-up	12.3	12.0	10.2 [32], 11.0 [13], 15.0 [33]
$3s3p^55s$	5.2(12)	2.3					
All	2.3(14)	100			100		

where A_{im}^{DTA} is the primary direct RTA rate. The intermediate state Ar^{*3+} autoionizes to the Ar⁴⁺ states with the rate of A_{mf}^{SA} and its total width is represented as Γ_m .

In this paper, the rates of the RSA decay were calculated using the AUGER component of the RATIP package [18], based on the multiconfiguration Dirac-Fock (MCDF) method [28] implemented in the GRASP2K program [29]. In the MCDF method, the single-electron orbitals and atomic state functions (ASFs) can be optimized by self-consistency procedures, which is accompanied by composing of all configuration state functions (CSFs) that interact with ASFs to include the electron correlation. The autoionizing rates and collision ionization strengths, based on distorted wave approximation, as well as the overlap integrals for calculating the RMA rates were obtained using the flexible atomic code [17] with some modifications [20].

III. RESULTS AND DISCUSSION

In this section we present calculated Auger rates and branching ratios (BRs) for specific configurations of final ions as well as the probabilities of the spectator, participator, and shake processes. These probabilities are obtained with a ratio of summation over all Auger rates that belong to a corresponding process to the total Auger rate. The Auger spectra are obtained by convolving the Auger rates with a Gaussian profile to take into account the instrument resolution and compared with experimental measurements obtained by multielectron coincidence spectroscopy [11]. Based on the energy resolving power $E/\Delta E \sim 60$ of the apparatus in Ref. [11], the constant full width at half maximum (FWHM) was chosen in a specific energy range of the Auger electron.

A. Resonant single Auger decay

The RSA decays are important for the resonant Auger decay of the Ar $2p_{3/2}^{-1}4s$, and their rates are crucial for resulting the RMA rates described in Sec. II. In the RSA decay, the shake process can be described as projecting the

initial wave function on one of the relaxed final ions. Therefore, in order to take into account the relaxation effect, the orbitals of the initial and final states should be optimized separately and are nonorthogonal. Stock *et al.* [30] proposed that many-electron single Auger amplitudes can be evaluated by employing a biorthonormal transformation for separately optimized orbitals. Then the additional contributions of the shake process are automatically considered via the mixing of different configurations. To apply a biorthonormal transformation to the atomic states between initial state Ar $2p_{3/2}^{-1}4s$ and final Ar⁺ states, the GRASP2K program [29] was applied (for details refer to Ref. [31]).

For describing the spectator, participator, and shake processes in the primary RSA decay of the Ar $2p_{3/2}^{-1}4s$, the interaction among the states belonging to the configurations $3s^23p^5$, $3s3p^6$, $3s^23p^4nl$, $3s3p^5nl$, and $3p^6nl$ ($nl = 3d, 4s, 4p, 4d, 5s, 5d, 6s, 6d, \text{ and } 7s$) is included for the Ar⁺ ion. Here, the final states with shaken $4p$ orbital are also included, which refers to a conjugate shake process due to a change in the parity of the initial Rydberg electron $4s$. Furthermore, some of the final states lying above the Ar²⁺ threshold can decay further via the emission of another Auger electron, which leads to the cascade RDA decay. Since such autoionizing states are affected strongly by electron correlation, the larger-scale CSFs produced by single and double excitations from the reference configurations $3s^23p^5$ and $3s3p^6$ to the orbitals $4s, 3d, 5s, \text{ and } 4p$ are also included.

Table I gives the calculated rates and BRs for main configurations in the Ar⁺ ion as well as the probabilities of the spectator, participator, and shake processes for the RSA decay of the Ar $2p_{3/2}^{-1}4s$, and the calculated probability of the shake-up $4s \rightarrow 5s$ process is consistent with available theoretical [32] and experimental [13,32,33] results. The spectator process that leaves the $4s$ electron in its Rydberg orbital significantly dominates with the probability of 71.7%, while the participator decay is quite weak with that of 0.3%. The probability of the shake-down process to the $3d$ subshell is estimated to be 15.4% and is greater than that of the shake-up $4s \rightarrow 5s$ process (12.3%), which is attributed to the

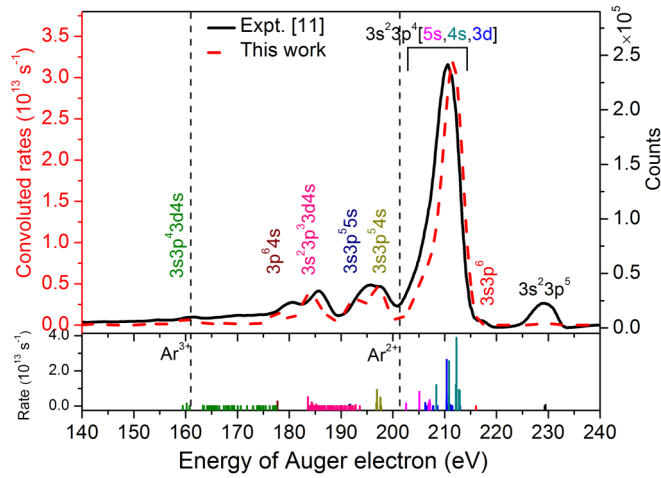


FIG. 1. Theoretical and experimental [11] resonant single Auger electron spectra for the Ar $2p_{3/2}^{-1}4s$. The theoretical spectra were shifted 1.8 eV toward low Auger energies. The vertical solid lines below the plots indicate the possible transitions, where the colors correspond to different final-state configurations that are associated with the spectator ($4s$ orbital), participator (only $3s$ and $3p$ orbitals), shake-down ($3d$ orbital), and shake-up ($5s$ orbital) processes. The two vertical dashed lines at 201.1 and 161.0 eV represent the double and triple-ionization thresholds, respectively.

strong mixing of the final ionic states between $3s^2 3p^4 4s$ and $3s^2 3p^4 3d$.

The RSA spectra were obtained by convolving the rates with a Gaussian profile of a 3.5-eV FWHM in Fig. 1, and agree with the experimental spectra [11]. The possible transitions with rates are indicated by the solid vertical lines below the plots, where the colors correspond to the configurations

of the final Ar^+ ion that are associated with the spectator ($4s$ orbital), participator (only $3s$ and $3p$ orbitals), shake-down ($3d$ orbital), and shake-up ($5s$ orbital) processes. It is found that the main peak at about 200–215 eV originates from the states $3s^2 3p^4 3d$, $3s^2 3p^4 4s$, and $3s^2 3p^4 5s$, and the contributions of $3s^2 3p^4 4s$ are most important due to the spectator process. The calculated intensities of the $3s^2 3p^5$ from the participator process look small compared with the experimental measurements; however, it should be noted that these experimental intensities could be attributed dominantly to valence photoionization [11]. Furthermore, the shake-down and shake-up processes give rise to other peaks of the RSA spectra. In Fig. 1, the states Ar^{*+} lying above Ar^{2+} and Ar^{3+} thresholds represented by the dashed vertical lines will decay further via the cascade RDA and RTA decays, respectively. However, as the populations of Ar^{*+} states lying above the triple-ionization threshold are rather small, the cascade RTA decays are negligible due to such Ar^{*+} states. Therefore, it is reasonable to neglect the cascade process described by Eq. (14) in Sec. II C for dealing with the RTA decays of the Ar $2p_{3/2}^{-1}4s$.

B. Resonant double Auger decay

The calculated Auger rates, the BRs for main configurations, as well as the probabilities of the spectator, participator, and shake processes including the cascade and direct processes are given in Table II for the RDA decay of the Ar $2p_{3/2}^{-1}4s$.

For the direct RDA decay, the contributions of the KO mechanism are much greater than those of the SO by an order of magnitude in Table II. This indicates that the KO mechanism is dominant, which is consistent with a recent experimental finding [10]. The SO can be also referred to

TABLE II. Rates (A^2) and branching ratios (BR^2) for main configurations in Ar^{2+} ions, as well as probabilities (P^2) of the spectator, participator, and shake processes including the cascade and direct processes of the resonant double Auger (RDA) decay. The KO and SO indicate the contributions from the knock-out and shake-off mechanisms, respectively, for the direct RDA decay. The numbers in brackets represent powers of 10.

Ar ²⁺	A^2 (s ⁻¹)					BR^2 (%)			Final orbital	Process	P^2 (%)		
	Direct			Cascade	RDA	Direct	Cascade	RDA			Direct	Cascade	RDA
	KO	SO	Total										
$3s^2 3p^4$	2.4(12)	8.6(10)	2.5(12)	4.5(13)	4.8(13)	9.0	83.3	58.2	$3s/3p$	Participator	9.7	96.6	67.1
$3s 3p^5$	1.9(11)	1.1(10)	2.0(11)	7.0(12)	7.2(12)	0.7	13.0	8.7					
$3p^6$	6.8(8)	4.2(7)	7.2(8)	1.5(11)	1.5(11)	~0	0.3	0.2					
$3s^2 3p^3 3d$	5.9(12)	2.9(11)	6.2(12)	3.5(11)	6.6(12)	22.2	0.6	8.0	$3d$	Shake-down	27.2	0.8	9.8
$3s 3p^4 3d$	1.3(12)	9.0(10)	1.4(12)	1.0(11)	1.5(12)	5.0	0.2	1.8					
$3p^5 3d$	1.1(10)	7.7(8)	1.2(10)	~0	1.2(10)	~0	~0	~0					
$3s^2 3p^3 4s$	1.1(13)	4.9(11)	1.1(13)	1.1(12)	1.2(13)	39.4	2.0	14.5	$4s$	Spectator	51.0	2.5	18.7
$3s 3p^4 4s$	3.0(12)	2.2(11)	3.2(12)	2.8(11)	3.5(12)	11.5	0.5	4.2					
$3p^5 4s$	2.9(10)	1.8(9)	3.0(10)	~0	3.0(10)	0.1	~0	~0					
$3s^2 3p^3 5s$	2.5(12)	1.2(11)	2.6(12)	2.0(10)	2.6(12)	9.3	~0	3.2	$5s$	Shake-up	12.1	~0	4.3
$3s 3p^4 5s$	7.3(11)	5.5(10)	7.9(11)	6.4(9)	8.0(11)	2.8	~0	1.1					
$3p^5 5s$	6.9(9)	5.2(8)	7.5(9)	~0	7.5(9)	~0	~0	~0					
All	2.7(13)	1.4(12)	2.8(13)	5.4(13)	8.2(13)	100	100	100			100	100	100

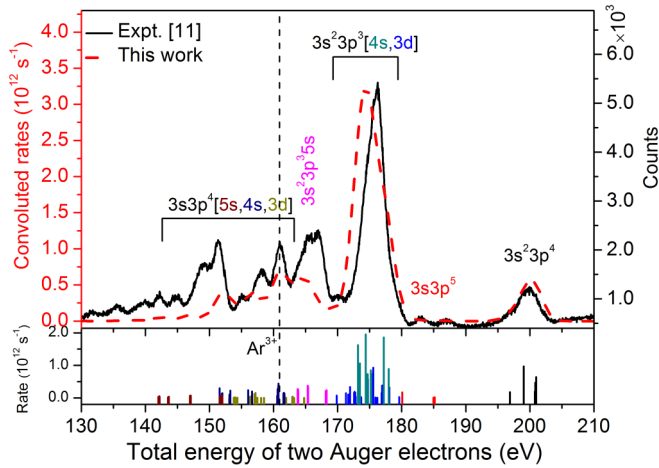


FIG. 2. Theoretical and experimental [11] direct resonant double Auger electron spectra for the $\text{Ar } 2p_{3/2}^{-1} 4s$. The vertical solid lines below the plots indicate the possible transitions, where the colors correspond to different final-state configurations that are associated with the spectator ($4s$ orbital), participator (only $3s$ and $3p$ orbitals), shake-down ($3d$ orbital), and shake-up ($5s$ orbital) processes. The vertical dashed line at 161.0 eV represents the triple-ionization threshold.

as the shake process of $4s \rightarrow \varepsilon l$, where εl represents the continuum electron instead of the bound one, in the RSA decay. Compared to the shake-up and shake-down processes in Table I, the SO is rather weak with the probability of 0.6% .

In the direct RDA decay, the most important transition originates from the configuration $3s^2 3p^3 4s$ with the rate of $1.1 \times 10^{13} \text{ s}^{-1}$ resulting in the BR of 39.4% . Then the spectator process dominates in the direct RDA decay with the probability of 51% . Due to the strong mixing with $3s^2 3p^3 4s$, the next strongest channel is from the configuration $3s^2 3p^3 3d$ with the rate of 6.2×10^{12} and accounts for the BR of 22.2% . Then the shake-down process to the $3d$ orbital with the probability of 27.2% dominates over the shake-up process to the $5s$ orbital with that of 12.1% , which indicates that the shake processes in the direct RDA decay are obviously more significant than those of core-ionized states such as $\text{C}^{-1} 1s^{-1}$ [34], $\text{Ne } 1s^{-1}$ [25,35], and $\text{Ar } 2p^{-1}$ [24,36]. Additionally, the contribution of the participator process is relative weak with the probability of 9.7% .

The calculated direct RDA spectra convoluted with a Gaussian profile of a 3.0 -eV FWHM are compared with the experimental spectra [11] in Fig. 2. It is found that the theoretical intensities reproduce all main structures of the experimental spectra, which could reveal the contributions from the spectator, participator, and shake processes. The vertical line at 161.0 eV represents the triple-ionization threshold. The states produced by the direct RDA decay that lie energetically above this threshold will autoionize further into Ar^{3+} states via the cascade RTA decay.

Apart from the direct RDA decays, the Ar^{2+} states can be populated via the cascade processes through the autoionization of intermediate autoionizing Ar^{*+} states produced by the primary RSA decays. In Table II, the $\text{Ar } 2p_{3/2}^{-1} 4s$ most preferentially decays into states $3s^2 3p^4$ and $3s3p^5$ with the

rates of 4.5×10^{13} and $7.0 \times 10^{12} \text{ s}^{-1}$, respectively, resulting in the participator process probability of 96.6% . Contrary to the direct process, the participator process dominates and the spectator and shake processes are weak in the cascade process.

For the total RDA decay, the direct and cascade processes with the rates of 2.8×10^{13} and $5.4 \times 10^{13} \text{ s}^{-1}$, respectively, result in the total RDA rate of $8.2 \times 10^{13} \text{ s}^{-1}$ in Table II. Then the Ar^{2+} ion yield produced by the RDA decays is determined to be 31.0% , which agrees well with the experimental values of 28% [11] and 30% [9]. Our results reveal that the cascade process is dominant with the contribution of 66% to the total RDA decay, which is consistent with the experimental estimation of $\sim 60\%$ [11]. The intermediate autoionizing states Ar^{*+} are often populated due to the spectator and shake processes in the primary RSA decay; as a consequence, the cascade processes are more favored in the RDA decay. This differs from the case of the core-ionized $\text{Ar } 2p^{-1}$, in which the cascade processes account for only $26 \pm 4\%$ of the total double Auger decay [36].

As shown in Table II, since the states belonging to the configuration $3s^2 3p^4$ are most populated accounting for the BR of 58.2% , the participator processes resulting in the configurations $3s^2 3p^4$, $3s3p^5$, and $3p^6$ are favored with the probability of 67.1% during the total RDA decay. The next most populated states are due to the configuration $3s^2 3p^3 4s$ with the BR of 14.5% , which suggests the spectator process with the probability of 18.7% . Furthermore, the contributions of the shake-down $4s \rightarrow 3d$ and shake-up $4s \rightarrow 5s$ process probabilities of 9.8 and 4.3% , respectively, are still not negligible for the populations of the final Ar^{2+} states. This indicates that the influence of shake processes on the formations of final states is distinctly enhanced for the core-excited $\text{Ar } 2p_{3/2}^{-1} 4s$ compared to the core-ionized cases such as $\text{Ne } 1s^{-1}$ [35], $\text{Ar } 2p^{-1}$ [24,27,36–38], and $\text{Kr } 3d^{-1}$ [39,40]. The theoretical RDA spectra (3.0 -eV FWHM) by including the cascade and direct processes, along with the experimental measurement [11], are shown in Fig. 3. It is found that the calculated intensities with inclusions of the spectator, participator, and shake processes are in general agreement with experimental data [11].

C. Resonant triple Auger decay

The characteristic data on the RTA decays of the $\text{Ar } 2p_{3/2}^{-1} 4s$ are listed in Table III. For the direct RTA decay, the most preferential configuration $3s^2 3p^3$ accounts for the BR of 43.6% with the rate of $2.8 \times 10^{12} \text{ s}^{-1}$, and the next one originates from $3s^2 3p^2 4s$ with the BR of 15.6% . Then the participator process forming the states of $3s^2 3p^3$ and $3s3p^4$ with the probability of 51.2% is more favored than the spectator process forming the states of $3s^2 3p^2 4s$ and $3s3p^3 4s$ with that of 26.5% , which means that the participator process becomes important, compared to the direct RDA decay discussed in Sec. III B. Furthermore, the shake-down $4s \rightarrow 3d$ and shake-up $4s \rightarrow 5s$ processes are also important with the probability of 16.8 and 5.4% , respectively. However, the contributions of the shake processes are limited for the core-ionized $\text{Ar } 2p^{-1}$ according to the triple Auger spectra [27], where the direct process is dominant. In Fig. 4, the calculated direct RTA

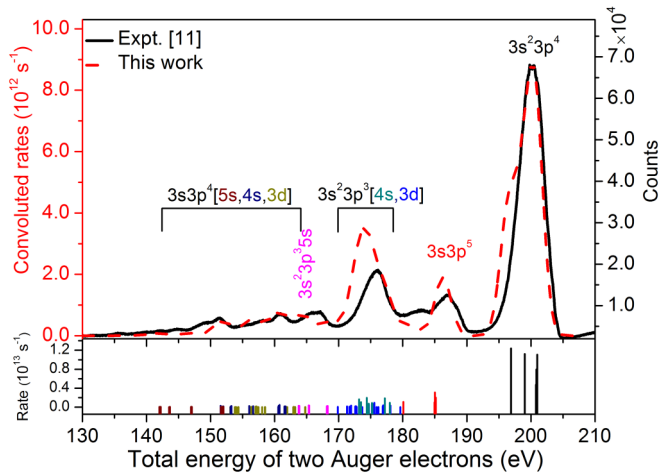


FIG. 3. Theoretical and experimental [11] resonant double Auger electron spectra with inclusion of the cascade and direct processes for the Ar $2p_{3/2}^{-1} 4s$. The vertical solid lines below the plots indicate the possible transitions, where the colors correspond to different final-state configurations that are associated with the spectator ($4s$ orbital), participator (only $3s$ and $3p$ orbitals), shake-down ($3d$ orbital), and shake-up ($5s$ orbital) processes.

spectra convolved with a Gaussian profile of a 2.5-eV FWHM agree well with the experimental measurements [11].

In the cascade RTA decay, the state Ar $2p_{3/2}^{-1} 4s$ decays preferentially into the final states of the configuration $3s^2 3p^3$ in the Ar $^{3+}$ ion, while the formations of the configurations $3s 3p^4$ and $(3s 3p)^4 nl$ ($nl = 3d, 4s$ and $5s$) are negligible.

The total RTA rate is determined to be $9.6 \times 10^{12} \text{ s}^{-1}$ by inclusions of the direct and cascade processes with that of 6.4×10^{12} and $3.2 \times 10^{12} \text{ s}^{-1}$, respectively. Therefore, the Ar $^{3+}$ ion yield due to RTA decay is determined to be 3.6%, which agrees with the experimental data of 3% [11] and 4% [9]. The calculated direct RTA decay is dominant, accounting for 67% of the total RTA decay, which is consistent with the experimental estimation of $\sim 60\%$ [11]. This is contrary to the total RDA decay, where the cascade processes are

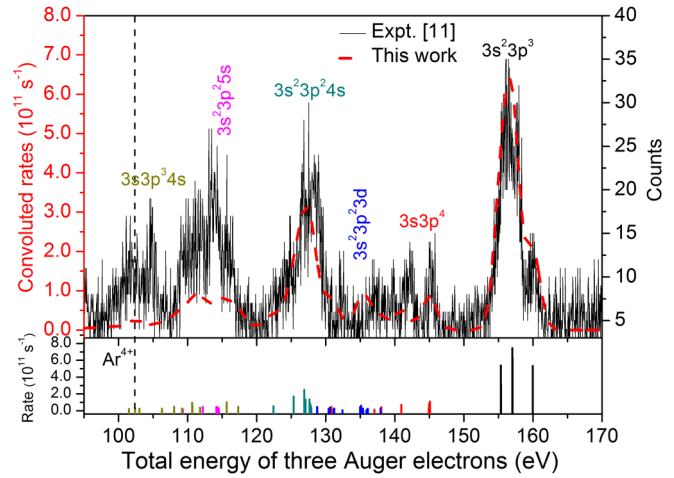


FIG. 4. Theoretical and experimental [11] direct resonant triple Auger electron spectra for the Ar $2p_{3/2}^{-1} 4s$. The vertical solid lines below the plots indicate the possible transitions, where the colors correspond to different final-state configurations that are associated with the spectator ($4s$ orbital), participator (only $3s$ and $3p$ orbitals), shake-down ($3d$ orbital), and shake-up ($5s$ orbital) processes. The vertical dashed line at 102.2 eV represents the quadruple-ionization threshold.

more favored. In the total RTA decay, the states belonging to the configuration $3s^2 3p^3$ are most populated with the BR of 62.4% and, hence, the participator process is dominant with the probability of 67.5%. The next most populated state is due to the configuration $3s^2 3p^2 4s$ with the BR of 10.4%, which results in the spectator process with the probability of 17.7%. Furthermore, the shake-down $4s \rightarrow 3d$ process with the probability of 11.3% is greater than shake-up $4s \rightarrow 5s$ process with that of 3.6%, which should not be neglected for the total RTA decay. However, the contributions of the shake processes are small for the triple Auger decay of core-ionized states such as C $1s^{-1}$ [34], Ne $1s^{-1}$ [35], and Ar $2p^{-1}$ [27].

The theoretical RTA spectra with a Gaussian profile of a 2.5-eV FWHM are shown in Fig. 5, which reproduce reasonably the relative intensities of the experimental spectra [11].

TABLE III. Rates (A^3) and branching ratios (BR^3) for main configurations in Ar $^{3+}$ ions, as well as probabilities (P^3) of the spectator, participator, and shake processes including the cascade and direct processes of the resonant triple Auger decay. The numbers in brackets represent powers of 10.

Ar $^{3+}$	A^3 (s^{-1})			BR^3 (%)			Final orbital	Process	P^3 (%)		
	Direct	Cascade	RTA	Direct	Cascade	RTA			Direct	Cascade	RTA
$3s^2 3p^3$	2.8(12)	3.2(12)	6.0(12)	43.6	100	62.4	$3s/3p$	Participator	51.2	100	67.5
$3s 3p^4$	4.9(11)	~ 0	4.9(11)	7.6	~ 0	5.1					
$3s^2 3p^2 3d$	6.6(11)	~ 0	6.6(11)	10.3	~ 0	6.9	$3d$	Shake-down	16.8	~ 0	11.3
$3s 3p^3 3d$	4.2(11)	~ 0	4.2(11)	6.5	~ 0	4.4					
$3s^2 3p^2 4s$	1.0(12)	~ 0	1.0(12)	15.6	~ 0	10.4	$4s$	Spectator	26.5	~ 0	17.7
$3s 3p^3 4s$	7.0(11)	~ 0	7.0(11)	10.9	~ 0	7.3					
$3s^2 3p^2 5s$	2.8(11)	~ 0	2.8(11)	4.4	~ 0	2.9	$5s$	Shake-up	5.4	~ 0	3.6
$3s 3p^3 5s$	6.5(10)	~ 0	6.5(10)	1.0	~ 0	0.7					
All	6.4(12)	3.2(12)	9.6(12)	100	100	100			100	100	100

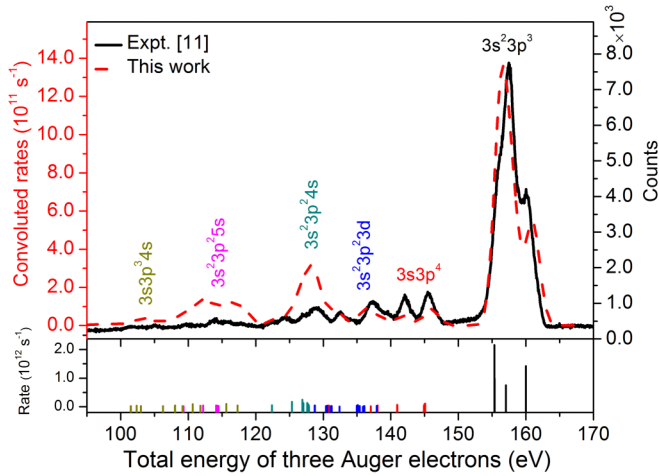


FIG. 5. Theoretical and experimental [11] resonant triple Auger electron spectra with inclusion of the cascade and direct processes for the Ar $2p_{3/2}^{-1} 4s$. The vertical solid lines below the plots indicate the possible transitions, where the colors correspond to different final-state configurations that are associated with the spectator ($4s$ orbital), participator (only $3s$ and $3p$ orbitals), shake-down ($3d$ orbital), and shake-up ($5s$ orbital) processes.

D. Resonant quadruple Auger decay

The resonant core-excited Ar $2p_{3/2}^{-1} 4s$ state that lies above the Ar⁴⁺ ground configuration $3s^2 3p^2$ can decay with four-electron emission as observed in the experiments [9,11]. To the best of our knowledge, there is no theoretical effort to interpret the RQA decay of the Ar $2p_{3/2}^{-1} 4s$ at present, especially for the direct processes. Here, we propose an approach described in Sec. IID by extending the KO and cascade mechanisms to deal with this RQA decay.

Figure 6 shows the calculated RQA spectra with a Gaussian profile of a 1.5-eV FWHM, which is in agreement with the experimental spectra [11].

The RQA rates are determined to be 2.2×10^{11} and $2.7 \times 10^{10} \text{ s}^{-1}$ for the direct and cascade processes, respectively, resulting in the total rate of $2.5 \times 10^{11} \text{ s}^{-1}$. The Ar⁴⁺ ion yield is determined to be 0.09% by including the direct (0.08%) and cascade (0.01%) processes, which agrees with the available experimental results of 0.03% [11] and 0.2% [9]. Our results indicate that the contribution of the direct process is far greater than that of the cascade one. Since the Ar^{*3+} states that lie above the quadruple-ionization threshold and decay further to the states Ar⁴⁺ are barely populated by the direct RTA decay as shown in Fig. 4, they are responsible for the weak cascade process. In Fig. 6, the participator process forming the $3s^2 3p^2$ states is favored, and the contributions of the spectator and shake processes are small.

E. Ion yields

The calculated ion yields of Ar⁺, Ar²⁺, Ar³⁺, and Ar⁴⁺ ions produced by the RSA, RDA, RTA, and RQA decays, respectively, of the Ar $2p_{3/2}^{-1} 4s$ including the cascade and direct processes are summarized in Table IV and in agreement with the available experimental values [9,11]. It should be noted that the experimental ion yields of Ref. [9] are deduced

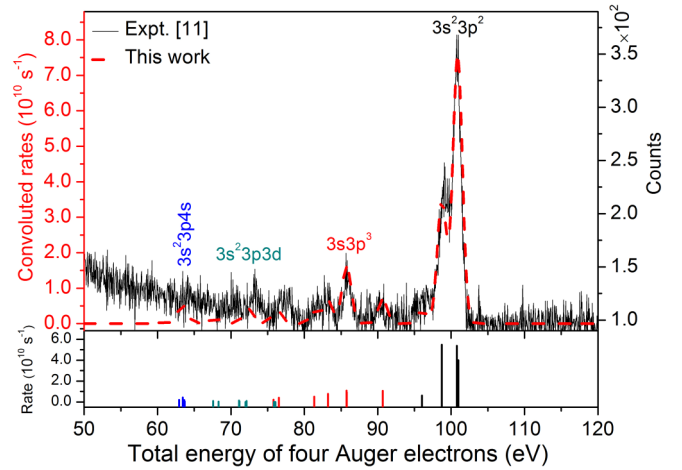


FIG. 6. Theoretical and experimental [11] resonant quadruple Auger electron spectra with inclusion of the cascade and direct processes for the Ar $2p_{3/2}^{-1} 4s$. The theoretical spectra were shifted 1.5 eV toward low Auger energies. The vertical solid lines below the plots indicate the possible transitions, where the colors correspond to different final-state configurations that are associated with the spectator ($4s$ orbital), participator (only $3s$ and $3p$ orbitals), and shake-down ($3d$ orbital) processes.

from the partial cross sections obtained from the mass spectrometry. The calculated ion yield of 10.6% for the direct RDA decay is close to that of $13 \pm 2\%$ [36], 13% [37], and 15% [38] for the double Auger decay of the core-ionized Ar $2p^{-1}$, for which the direct processes are mainly dominant [36]. However, if the cascade processes are included, the ion yield produced by the RDA decay of Ar $2p_{3/2}^{-1} 4s$ is roughly twice greater than that of the core-ionized Ar $2p^{-1}$, which mainly results from the significant spectator and shake processes due to the Rydberg electron $4s$. The ion yield produced by the RTA decay of the core-excited Ar $2p_{3/2}^{-1} 4s$ is far greater than that of 0.18% [24,27] and $0.3 \pm 0.1\%$ [37] after the triple Auger decay of the core-ionized Ar $2p^{-1}$, which also shows the importance of the initial Rydberg electron $4s$. Therefore, in contrast to core-ionized states, the enhancement of the ion yields during the RMA decay is expected due to the presence of the initial Rydberg electron.

Our results in Table IV imply that the contributions of the direct process become dominant with the increase of

TABLE IV. Ion yields (in percentages) produced by the resonant single, double, triple, and quadruple Auger decays represented by the RSA, RDA, RTA, and RQA, respectively, of the Ar $2p_{3/2}^{-1} 4s$. The calculated ion yields in the fifth column with the inclusions of the cascade and direct processes are compared with experimental data [9,11].

Ions	Decays	This paper			Expt.	
		Cascade	Direct	Total	Ref. [11]	Ref. [9]
Ar ⁺	RSA			65.3	69	66
Ar ²⁺	RDA	20.4	10.6	31.0	28	30
Ar ³⁺	RTA	1.2	2.4	3.6	3	4
Ar ⁴⁺	RQA	0.01	0.08	0.09	0.03	0.2

the number of emitted Auger electrons, as observed in the experiment [11].

IV. CONCLUSIONS

The RMA decays following the resonant $2p_{3/2} \rightarrow 4s$ photoexcitation in neutral argon are investigated theoretically. The rates of the RMA decays are evaluated by using multistep approaches, namely, the cascade, KO, and SO mechanisms within the framework of MBPT. According to the calculated rates, the BRs of the different configurations as well as the probabilities of the spectator, participator, and shake processes are obtained; moreover, the contributions from the direct and cascade processes are determined as well. The calculated Auger spectra are in general agreement with the experimental measurements [11]. Furthermore, the calculated ion yields produced by the RSA, RDA, RTA, and RQA decays are in agreement with experimental data [9,11].

Our results indicate that the contributions of the direct processes become dominant with increasing the number of the emitted electrons. In the direct RMA decay, the spectator processes are predominant, while the contributions of the

participator processes become more important as the number of the emitted Auger electrons increases. Additionally, the contributions of the shake processes are found to be important in the direct process, whereas they are usually limited for the cases of core-ionized states such as C $1s^{-1}$ [34], Ne $1s^{-1}$ [35], and Ar $2p^{-1}$ [27]. In contrast to the case of core-ionized state Ar $2p^{-1}$ [24,27,36–38], the ion yields are enhanced with inclusion of the cascade and direct processes for the total RMA decays of the Ar $2p_{3/2}^{-1}4s$, which indicates that the spectator and shake processes play an essential role in the RMA decay.

ACKNOWLEDGMENTS

We would like to thank Y. Hikosaka for providing the experimental data from Ref. [11]. This work is supported by the National Key Research and Development Program of China (Grant No. 2017YFA0402300), the National Natural Science Foundation of China (Grants No. 11774344 and No. 11474033), and the Joint Foundation of the National Natural Science Foundation and the China Academy of Engineering Physics (Grant No. U1330117).

-
- [1] F. Da Pieve, L. Avaldi, R. Camilloni, M. Coreno, G. Turri, A. Ruocco, S. Fritzsche, N. M. Kabachnik, and G. Stefani, *J. Phys. B* **38**, 3619 (2005).
- [2] N. Stolterfoht, C. C. Havener, R. A. Phaneuf, J. K. Swenson, S. M. Shafroth, and F. W. Meyer, *Phys. Rev. Lett.* **57**, 74 (1986).
- [3] H. Fukuzawa, S.-K. Son, K. Motomura, S. Mondal, K. Nagaya, S. Wada, X.-J. Liu, R. Feifel, T. Tachibana, Y. Ito, M. Kimura, T. Sakai, K. Matsunami, H. Hayashita, J. Kajikawa, P. Johnsson, M. Siano, E. Kukk, B. Rudek, B. Erk, L. Foucar, E. Robert, C. Miron, K. Tono, Y. Inubushi, T. Hatsui, M. Yabashi, M. Yao, R. Santra, and K. Ueda, *Phys. Rev. Lett.* **110**, 173005 (2013).
- [4] L. Young, E. P. Kanter, B. Krässig, Y. Li, A. M. March, S. T. Pratt, R. Santra, S. H. Southworth, N. Rohringer, L. F. Dimauro, G. Doumy, C. A. Roedig, N. Berrah, L. Fang, M. Hoener, P. H. Bucksbaum, J. P. Cryan, S. Ghimire, J. M. Glowina, D. A. Reis, J. D. Bozek, C. Bostedt, and M. Messerschmidt, *Nature (London)* **466**, 56 (2010).
- [5] L. J. Frasinski, V. Zhaunerchyk, M. Mucke, R. J. Squibb, M. Siano, J. H. D. Eland, P. Linusson, P. v.d. Meulen, P. Salén, R. D. Thomas, M. Larsson, L. Foucar, J. Ullrich, K. Motomura, S. Mondal, K. Ueda, T. Osipov, L. Fang, B. F. Murphy, N. Berrah, C. Bostedt, J. D. Bozek, S. Schorb, M. Messerschmidt, J. M. Glowina, J. P. Cryan, R. N. Coffee, O. Takahashi, S. Wada, M. N. Piancastelli, R. Richter, K. C. Prince, and R. Feifel, *Phys. Rev. Lett.* **111**, 073002 (2013).
- [6] G. Goldsztejn, T. Marchenko, R. Püttner, L. Journel, R. Guillemin, S. Carniato, P. Selles, O. Travnikova, D. Céolin, A. F. Lago, R. Feifel, P. Lablanquie, M. N. Piancastelli, F. Penent, and M. Simon, *Phys. Rev. Lett.* **117**, 133001 (2016).
- [7] J. A. Tanis, J.-Y. Chesnel, F. Frémont, D. Hennecart, X. Husson, A. Cassimi, J. P. Grandin, B. Skogvall, B. Sulik, J.-H. Bremer, and N. Stolterfoht, *Phys. Rev. Lett.* **83**, 1131 (1999).
- [8] D. V. Morgan, M. Sagurton, and R. J. Bartlett, *Phys. Rev. A* **55**, 1113 (1997).
- [9] J. A. R. Samson, W. C. Stolte, Z. X. He, J. N. Cutler, and D. Hansen, *Phys. Rev. A* **54**, 2099 (1996).
- [10] Y. Hikosaka, P. Lablanquie, F. Penent, P. Selles, T. Kaneyasu, E. Shigemasa, J. H. D. Eland, and K. Ito, *Phys. Rev. A* **80**, 031404(R) (2009).
- [11] Y. Hikosaka, P. Lablanquie, F. Penent, P. Selles, E. Shigemasa, and K. Ito, *Phys. Rev. A* **89**, 023410 (2014).
- [12] H. Aksela, *J. Electron Spectrosc. Relat. Phenom.* **72**, 235 (1995).
- [13] J. A. de Gouw, J. van Eck, A. C. Peters, J. van der Weg, and H. G. M. Heideman, *J. Phys. B* **28**, 2127 (1995).
- [14] H. Aksela and J. Mursu, *Phys. Rev. A* **54**, 2882 (1996).
- [15] S.-M. Huttula, S. Heinäsmäki, H. Aksela, M. Jurvansuu, and S. Aksela, *J. Phys. B* **34**, 2325 (2001).
- [16] B. Paripás, B. Palásthy, M. Štuhec, and M. Žitnik, *Phys. Rev. A* **82**, 032508 (2010).
- [17] M. F. Gu, *Can. J. Phys.* **86**, 675 (2008).
- [18] S. Fritzsche, *Comput. Phys. Commun.* **183**, 1525 (2012).
- [19] F. Zhou, Y. Ma, and Y. Qu, *Phys. Rev. A* **93**, 060501(R) (2016).
- [20] Y. Ma, F. Zhou, L. Liu, and Y. Qu, *Phys. Rev. A* **96**, 042504 (2017).
- [21] M. Ya. Amusia, I. S. Lee, and V. A. Kilin, *Phys. Rev. A* **45**, 4576 (1992).
- [22] S. L. Carter and H. P. Kelly, *Phys. Rev. A* **24**, 170 (1981).
- [23] T. Schneider, P. L. Chocian, and J.-M. Rost, *Phys. Rev. Lett.* **89**, 073002 (2002).
- [24] P. Lablanquie, L. Andric, J. Palaudoux, U. Becker, M. Braune, J. Viefhaus, J. H. D. Eland, and F. Penent, *J. Electron Spectrosc. Relat. Phenom.* **156–158**, 51 (2007).
- [25] J. Viefhaus, A. N. Grum-Grzhimailo, N. M. Kabachnik, and U. Becker, *J. Electron Spectrosc. Relat. Phenom.* **141**, 121 (2004).
- [26] Y.-K. Kim and M. E. Rudd, *Phys. Rev. A* **50**, 3954 (1994).
- [27] P. Lablanquie, M. A. Khalal, L. Andric, J. Palaudoux, F. Penent, J.-M. Bizau, D. Cubaynes, K. Jänkälä, Y. Hikosaka, K. Ito,

- K. Bučar, and M. Žitnik, *J. Electron Spectrosc. Relat. Phenom.* **220**, 125 (2017).
- [28] I. P. Grant, *Relativistic Quantum Theory of Atoms and Molecules* (Springer, New York, 2007).
- [29] P. Jönsson, X. He, C. Froese Fischer, and I. P. Grant, *Comput. Phys. Commun.* **177**, 597 (2007).
- [30] S. Stock, R. Beerwerth, and S. Fritzsche, *Phys. Rev. A* **95**, 053407 (2017).
- [31] J. Olsen, M. R. Godefroid, P. Jönsson, P. Å. Malmqvist, and C. F. Fischer, *Phys. Rev. E* **52**, 4499 (1995).
- [32] J. Mursu, H. Aksela, O.-P. Sairanen, A. Kivimäki, E. Nömmiste, A. Ausmees, S. Svensson, and S. Aksela, *J. Phys. B* **29**, 4387 (1996).
- [33] M. Meyer, E. Von Raven, M. Richter, B. Sonntag, and J. E. Hansen, *J. Electron Spectrosc. Relat. Phenom.* **51**, 407 (1990).
- [34] A. Müller, A. Borovik, Jr., T. Buhr, J. Hellhund, K. Holste, A. L. D. Kilcoyne, S. Klumpp, M. Martins, S. Ricz, J. Viefhaus, and S. Schippers, *Phys. Rev. Lett.* **114**, 013002 (2015).
- [35] Y. Hikosaka, T. Kaneyasu, P. Lablanquie, F. Penent, E. Shigemasa, and K. Ito, *Phys. Rev. A* **92**, 033413 (2015).
- [36] J. Viefhaus, S. Cvejanović, B. Langer, T. Lischke, G. Prümper, D. Rolles, A. V. Golovin, A. N. Grum-Grzhimailo, N. M. Kabachnik, and U. Becker, *Phys. Rev. Lett.* **92**, 083001 (2004).
- [37] S. Brünken, C. Gerth, B. Kanngießer, T. Luhmann, M. Richter, and P. Zimmermann, *Phys. Rev. A* **65**, 042708 (2002).
- [38] M. Nakano, Y. Hikosaka, P. Lablanquie, F. Penent, S. M. Huttula, I. H. Suzuki, K. Soejima, N. Kouchi, and K. Ito, *Phys. Rev. A* **85**, 043405 (2012).
- [39] E. Andersson, S. Fritzsche, P. Linusson, L. Hedin, J. H. D. Eland, J.-E. Rubensson, L. Karlsson, and R. Feifel, *Phys. Rev. A* **82**, 043418 (2010).
- [40] J. Palaudoux, P. Lablanquie, L. Andric, K. Ito, E. Shigemasa, J. H. D. Eland, V. Jonauskas, S. Kučas, R. Karazija, and F. Penent, *Phys. Rev. A* **82**, 043419 (2010).